REVISTA MATÉRIA V.26 N.04

ISSN 1517-7076 articles e13112, 2021

Effects of tin on the performance of ZnO photoanode for DSSC

Efeitos do estanho no desempenho dos fotoanodos de ZnO para CSSC

Vanja Fontenele Nunes[1], Francisco Marcone Lima[1], Edwalder Silva Teixeira[1], Paulo Herbert França Maia Júnior[1], Ana Fabíola Leite Almeida[2], Francisco Nivaldo Aguiar Freire[1]

[1] Universidade Federal do Ceará, Programa de Pós-Graduação em Engenharia e Ciências dos Materiais-Campus do Pici, 729, CEP: 60.440-554, Ceará, Fortaleza, Brasil.

[2] Universidade Federal do Ceará, Programa de Pós-Graduação em Engenharia Mecânica- Campus do Pici,714, CEP: 60.455-760, Ceará, Fortaleza, Brasil.

e-mail: vanjafnunes@gmail.com, marconeufc@gmail.com, edwalderteixeira@hotmail.com, phfmj2010@gmail.com, nivaldo@ufc.br, anafabiola@ufc.br

ABSTRACT

Tin Zinc Oxide thin films were deposited on transparent conductive oxide by chemical bath, at percentages of 5, 10 and 15% of tin (Sn) on the zinc oxide (ZnO) structure. All films were thermally treated to improve its crystallinity. The produced films with tin were characterized by x-ray diffraction and optical measurements, such as absorbance, transmittance and reflectance. The x-ray spectrum showed the formation of the ZnO wurtzite and the crystallite size of the films were calculated to be 53.74; 79.59 and 66.38 nm for the photoanodes at 5, 10 and 15% of tin (Sn), respectively, on the zinc oxide structure. The calculated band gap energy of the films revealed that the presence of tin can reduce the band gap energy to about 3.2 eV. Those films were used as photoanodes on dye sensitized solar cells (DSSC) to observe the effects of the tin (Sn) on the photovoltaic activity of the zinc oxide (ZnO) semiconductor. Parameters such as efficiency and short circuit current density were particularly affected by the presence of tin in the composition, with the 5% Sn ZnO film presenting the best results of 7.56 % efficiency and 34.35 mA/cm^2, short circuit current density, the other films presented lower values for efficiency, which can be attributed to lower values of short-current density.

Keywords: Zinc oxide, tin, solar cell.

RESUMO

Filmes de estanho/óxido de zinco foram depositados em óxido condutor transparente por banho químico, a porcentagens de 5, 10 e 15% de estanho (Sn) na estrutura de óxido de zinco (ZnO). Todos os filmes foram tratados termicamente para melhorar sua cristanilidade. Os filmes produzidos foram caracterizados por difração de raios x e medidas ópticas, como absorbância, transmitância e reflectância. O espectro de raios x mostrou a formação de ZnO na forma de wurtzite e os tamanhos dos cristalitos foram de 53,74; 79,59 e 66,38 nm para os fotoanodos a 5, 10 e 15% de estanho (Sn), respectivamente, na estrutura do óxido de zinco. Os valores calculados para a energia de banda proibida dos filmes revelaram que a presença de estanho pode reduzir o valor da energia até aproximadamente 3,2 eV. Esses filmes foram usados como fotoanodos em células solares sensibilizadas por corante (CSSC) para observar os efeitos do estanho (Sn) na atividade fotovoltaica do semicondutor de óxido de zinco (ZnO). Parâmetros como eficiência e densidade de corrente de curto- circuito foram particularmente afetados pela presença de estanho na composição, com o filme de ZnO a 5% de Sn apresentando os melhores resultados de 7,56% de eficiência e 34,35 mA/cm^2 de densidade de corrente de curto-circuito, os demais filmes apresentaram menores valores para a eficiência, o que pode ser atribuído aos menores valores alcançados para a corrente de curto circuito.

Palavras-chave: Óxido de zinco, estanho, célula solar.

Autor Responsável: Vanja Nunes Data de envio: 12/01/2021 Data de aceite: 07/06/2021

10.1590/S1517-707620210004.1312

1. INTRODUCTION

Growing energy demand has increased the interest for alternative and renewable forms of energy. Amongst them, solar energy occupies a prominent place, especially in places with abundant sources of sunlight. Dye sensitized solar cell (DSSC) assembled by O'Regan and Gratzel in 1991 is a device which converts sunlight into electrical energy, with advantages such as the possibility of being manufactured without clean room technology, low cost, and, also, it can be used between low light and full light conditions [1]. DSSC function is based on the electron excitation from a dye through a semiconductor, an external circuit and back to be recovered by a counter electrode and an electrolyte redox [2]. The semiconductor used must have properties such as transparency and electron mobility. Zinc oxide is an example of such a semiconductor, it has high transparency in the visible light due to its band gap value (about 3.4 eV), electron mobility of 115–155 (cm^2 V^{-1} s^{-1}) and it is a cost effective material [3]. However, its setbacks include fast recombination of the electron-hole pair and low absorption on the visible light spectrum [4]. The goal is to improve the efficiency of DSSC with ZnO. For that, many authors have been doping the ZnO structure, such as IWANTONO *et al.* (2018) [5]; SINHA *et al.* (2018) [6]; RAJAN and LOUIS (2020) [7], RAHMAN *et al.* (2019) [8] and KHADTARE *et al.* (2021) [9]. Tin (Sn) can improve the electrical conductivity of the zinc oxide thin film and can be used in the ZnO structure due to the lower radius of the Sn^{4+} ion (0.69 Å), compared to the Zn^{2+} ion (0.74 Å), that does not change the lattice of the oxide when used at lower percentages of doping [10]. Many authors have tested tin in the zinc oxide structure, OZGÜR, *et al.* (2019) [11] vacuum deposited large crystallites of ZnO thin films doped with Sn; THIRUMOORTHIA and PRAKASH (2019) [10] deposited (1 0 1) oriented tin zinc oxide thin films by spray pyrolysis and XU, *et al.* (2019) [12] increased the surface energy and photocatalytic activity of ZnO thin films by Sn ions doping.

In this work, it is reported the study of ZnO as semiconductor on a DSSC, decorated with tin, to improve the device efficiency, and, also, to investigate its morphological and optical characteristics when changing the percentage of tin in the ZnO composition.

2. MATERIALS AND METHODS

Three FTO (fluoride tin oxide) glasses were immersed into a 5 g/L aqueous solution of zinc oxide (Dinamica Ltda.). For the first sample, the solution had 5% (wt%) of $SnCl_2.2H_2O$ (Dinamica Ltda.), the second 10% (wt%) of tin chloride and, the third, 15% (wt%). Before immersion, the FTOs were cleaned in an ultrasonic bath for 30 minutes in acetone 99.5% (Qhemis) and ethyl alcohol (CEQUÍMICA). The three zinc oxide/tin chloride solutions also were in ultrasonic baths for 30 minutes before covering the FTO under the solution. Afterwards, the FTOs with the zinc oxide thin film deposited with tin were treated thermally at 450 °C for 30 minutes, each one.

The FTOs with the Sn:ZnO films were, then, used as the photoanodes in three dye-sensitized solar cells (DSSC), where platinum acted as the counter electrode, $I^-_3/3I^-$ was the redox pair electrolyte and the N719 was the ruthenium based dye. The films were immersed in a N719 alcohol ethylic solution ($3x10^{-4}$ mol/L) for 24 hours. All the reagents were used without further purification and the FTO glass, the electrolyte; the platinum and the ruthenium based dye were from Solaronix.

The DSSC assemblies were then tested in a potentiostat (AUTOLAB PGSTAT302N) Metrohm, at 100 mW/cm^2 light simulation, white neutral LED. The potentiostat generated the values of Jsc, and Voc and the other photovoltaic parameters for each cell. Also, the photoanodes were submitted to UV-Vis (Agilent Technologies- Cary Series) tests to obtain the optical characteristics in the spectrum range between 200 and 800 nm. The morphological characterization of the films was done through x-ray diffraction (Rigaku DMAXB with Cu-Kα).

3. RESULTS AND DISCUSSION

3.1 X-Ray Diffraction

The main peaks found from the XRD were at the diffraction planes (100), (002), (101), (102), (110) and (103) according to the ICSD card number 082028 (Figure 1). The observed peaks match the wurtzite hexagonal structure of the ZnO [13]. The preferential peak on all three was located at (101) direction, a sign of the polycrystalline nature of the structure [14]. The narrowing of the peaks reveals good crystallinity of the zinc oxide. From the XRD patterns, at 15% Sn, the intensity of the peaks decreased. This occurs due to the substitution of the Zn^{2+} ions for the Sn^{2+} ions, which have lower radius [15]. The addition of the Sn contributes to reduce the crystallinity of the ZnO film [16]. The reason for such may be the formation of stress on the crystalline structure due to the replacement of the ions [17]. Moreover, the crystallite size (D)

was calculated by the Scherrer equation ($D=k\lambda/\beta\cos\theta$), where k is taken as 0.9, λ is wavelength (1.5406 Å), β is the broadening of the diffraction line at half intensity and θ is the Bragg's diffraction angle [5]. The values of average crystallite sizes were 53.74, 79.59 and 66.38 nm, for the doping at 5, 10 and 15%, respectively. The larger values of the crystallite sizes are in accordance with the temperature of the thermal treatment, as reported elsewhere [14]. VISHWAS, *et al.* (2012) [18] also found Sn/ZnO crystallite sized average of 60 nm, as well as BEDIA *et al*, 2015 [19]. The lower D (nm) was found for the Sn-ZnO at 5% (Sn). Also, the presence of other peaks at 15% may indicate the formation of secondary Sn^{4+} phases [20].

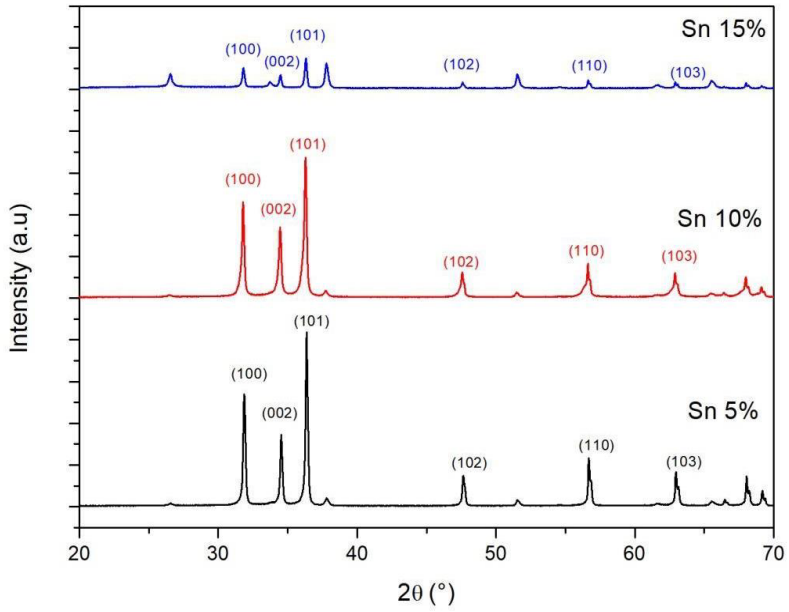

Figure 1: XRD diffraction planes for the three tested photoanodes (Source: Own author).

3.2 Optical Characterization

Figure 2 plots the absorbance values of the three tested photoanodes, in a wavelength range between 200 and 800 nm. The peaks were around the range between 300 and 400 nm, which are expected for the zinc oxide that absorbs in this range. However, it is possible to see that for the photoanode decorated at 5% tin, the peak was above the other two, at 10% and 15 %. This could have affected the photovoltaic performance for the solar cell assembled with the 5% tin decorated film photoanode. This behavior follows what THIRUMOORTHI and PRAKASH (2019) [10] observed, when increasing the tin percentage, from 0 to 8%. The red shift observed from about 300 nm to close 400 nm indicates the presence of Sn ions on the ZnO structure [15].

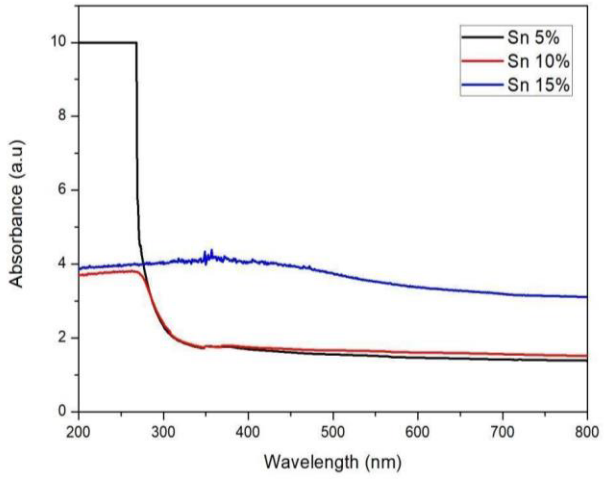

Figure 2: Absorbance spectra for the three photoanodes (Source: Own author)

The spectrum for transmittance is plotted in Figure 3. The highest value of Sn (15 %wt) had the lowest transparency on the visible range. This trend was also observed by other authors [12]; who, by increasing the percentage of Sn in the film, had lower transparency. AJILI, *et al.* (2013) [17] suggests that the transmittance of the ZnO layer decreases for higher tin percentage, due to the formation of a thicker layer that reduces the transmittance of the film. CHAHMAT, *et al.* (2012) [21] observed lower transmittance range when increasing the tin doping from 4% to 6% and 8%. GANESH, *et al*. (2017) [22] also observed a tendency for lower transmittance at higher tin load and indicates the thickness as the main reason for such an event. Additionally, the lower transmittance can indicate the scattering of the incident light that reaches the crystalline structure. As a consequence, the light scattering can be responsible for lower photocatalytic efficiency [14]. To verify the reason for the lower transparency, the reflectance spectra were plotted. It is seen, by Figure 4, that the scattering of the light caused the higher reflectance and, as consequence, lower transmittance. The lower reflectance for the 5% tin zinc oxide thin film (Figure 4) indicates that, for this film, there was a better internal path for the incident light, which favors the photocurrent activity [14]. The low reflectance is a characteristic of thin films, and it was found using the relation on KHELLADI and SARI (2013) [23].

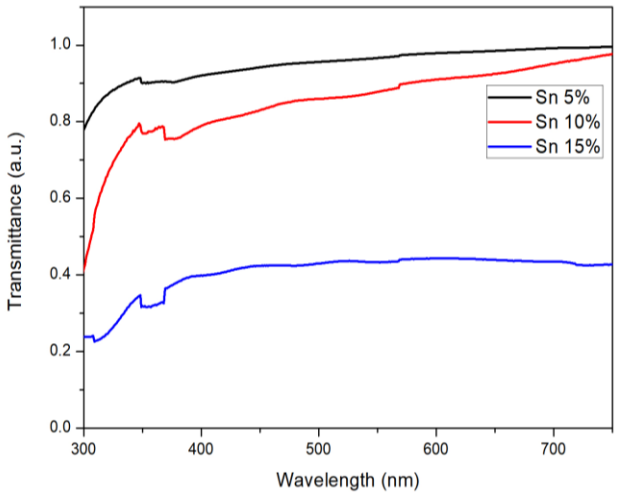

Figure 3: Transmittance spectra for the Sn/ZnO thin films (Source: Own author)

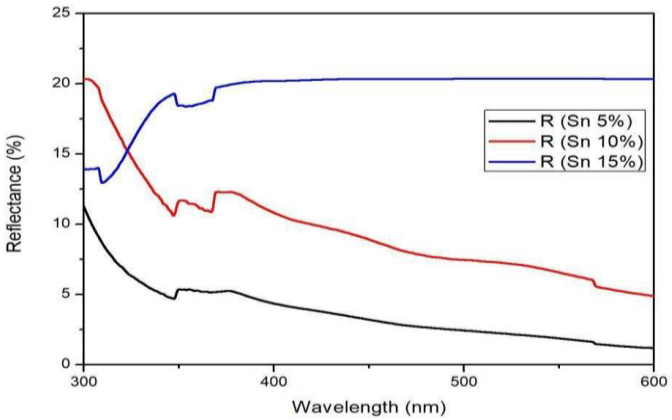

Figure 4: Reflectance spectra calculated for the thin films (Source: Own author)

The band gap energy (Eg) values were calculated using the modified Kubelka-Munk method, with uses values of $(F(R)*hv)^n$ versus (hv), where n=2 for indirect transition [24]. From the estimated band gap energy (Figure 5), it is possible to understand that the cell with the 5% tin oxide had the best efficiency values, possibly due to its low band gap energy, compared to the other two oxides semiconductors, providing good electron transmission inside the cell. The estimated values for band gap were 3.2, 3.34 and 3.5 eV for 5%, 10% and 15% tin doping, respectively, following the pattern observed by other studies, GANESH, *et al.*

(2017) [22] observed values of 3.22 eV for 5% Sn doping on ZnO thin films, but, when increasing the doping to 7% the band gap value jumped to 3.34 eV, YILDIZ, *et al.* (2012) [13] also obtained the band gap energy values around 3.2 eV for 5% of tin on zinc oxide thin films. The increase of the band gap for higher Sn percentage can be explained by the higher tin concentration causing thicker films, which increases energy of band gap (Eg) values [22]. Also, it is known for Sn to have a Burstein-Moss effect, which causes carrier-induced alteration of band gap values [25]. Also, the thermal treatment at 450 °C helps to reduce the band gap values for ZnO thin films, as it is seen in KANNAN, *et al.* (2020) [26].

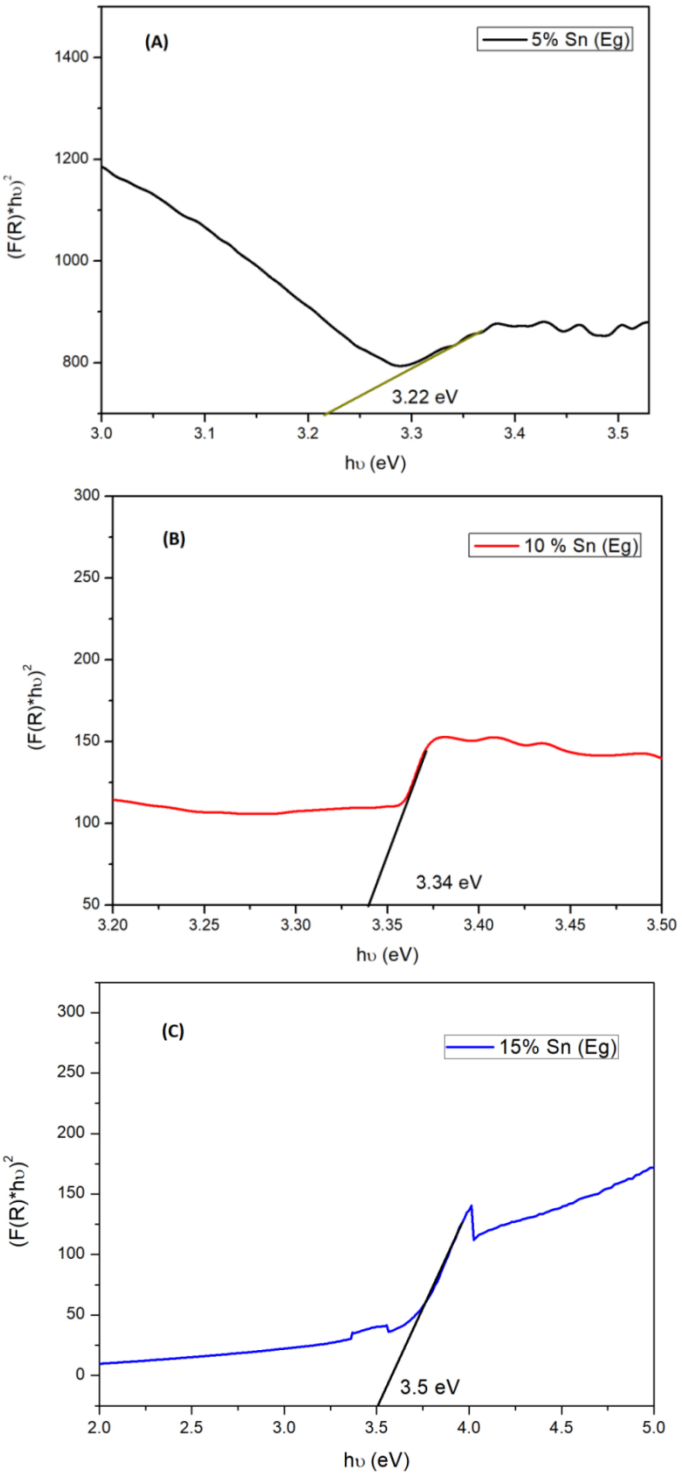

Figure 5: Modified Kubelka-Munk method for the Sn/ZnO photoanodes band gap values at (A) 5% Sn (B) 10% Sn and (C) 15% Sn (Source: Own author).

3.2 Photovoltaic Performance

The values for current density versus potential were plotted in Figure 6, for the cells tested under 100 mW/cm^2 light simulation. The short-current density at 5% Sn, observed from the figure, is placed way above the remaining two others. It can be verified that the lower current density at 10% is almost 7 times less than the highest value of short-circuit current density (Jsc). It is seen that the influence of tin on the values of Jsc must be limited to doping concentrations below 10%, because, at higher values, the Jsc of the photoanodes are closer to the values of undoped films [15].

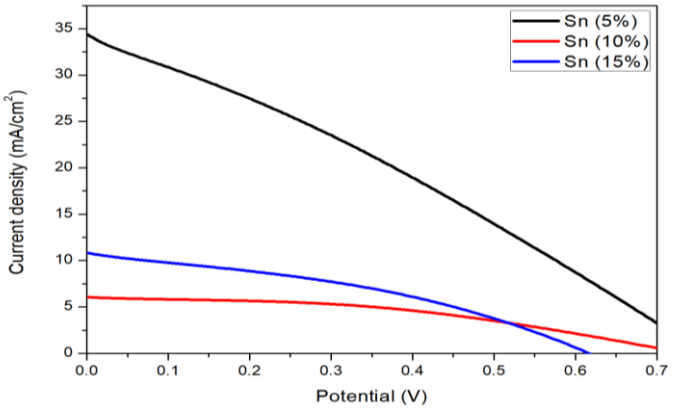

Figure 6: J-V curves of the photoanodes (5, 10 and 15% Sn) (Source: Own author).

Table 1 summarized the photovoltaic parameters for the three cells assembled with the Sn/ZnO photoanodes. As it is observed by the data, the photoanode at 5% tin had the best results for efficiency (□), photocurrent density (Jsc) and open circuit voltage (Voc). YE, *et al.* (2010) [27] also observed improvement of 105% on the Jsc of DSSC via Sn doping on ZnO/FTO. The presence of Sn particles into the ZnO is known to improve the photo-excited electron transportation under sunlight, resulting in higher current-density, which leads to improved photovoltaic efficiency (□) [15]. One of the parameters that can explain this good performance is the low value of series resistance (Rs) which favors the electron passage through the circuit, besides a low value for the shunt resistance (Rsh). The highest value of series resistance for the DSSC at 10% Sn can help to understand the lower photovoltaic efficiency. This resistance could have been caused by the formation of Zn^{2+}/dye particles aggregation, which stops the transportation of the excited electrons [3]. This aggregation also reduces the specific surface area, which affects the efficiency of the cell [28]. ROY et al. (2021) [29], reaffirms this theory, according to whom, to maximize the photochemical properties of the photoanode, it is necessary to optimize the dye loading, avoiding the formation of aggregates. Also, the size of the crystallite for the 10% Sn photoanode, 79.59 nm, may have contributed to the increase in resistance for the excited electron. Optimum values for crystallite size help to absorb the dye on the film structure, but when the size (D) is too high, it hinders the electron transportation process. Additionally, the DSSC at 10% presented photovoltaic values close to the ones verified for the undoped ZnO nanoparticles, at about 6 mA/cm^2, for Jsc, 1.97% efficiency (□) and 0.485, fill factor (FF) [30]. The high Voc on the photoanodes is due to the n-type doping nature of the Sn, which raises the Fermi level between the structure and the electrolyte [27]. The low fill factor (FF) obtained for the films can be explained by the time of dye soaking (24 h), observed sometimes for nanoparticles that are immersed on dye for longer periods of time [3]. It is clear, by the results, that the values of current density of the cells lead to better results of efficiency for the tested devices.

Table 1: Photovoltaic properties of the DSSCs with the three electrodes (Source: Own author)

	Jsc(mA/cm^2)	Voc(V)	FF	□ (%)	Rs (Ω/cm^2)	Rsh (Ω/cm^2)
Sn 5%	34.35	0.76	0.29	7.56	18.19	29.35
Sn 10%	6.06	0.73	0.42	1.86	54.22	438.52
Sn 15%	10.81	0.62	0.37	2.46	24.96	96.93

4. CONCLUSION

Tin zinc oxide thin films were successfully deposited on fluor doped tin oxide (FTO) at the concentrations of 5, 10 and 15% by chemical bath. The presence of 5 %(wt) tin reduced the usual band gap of the ZnO material (about 3.54 eV) to 3.2 eV. It helped to improve the photovoltaic parameters of the DSSC assembled cell using the Sn/ZnO thin film, especially the short circuit current values, 34.35 mA/cm^2 at 5% Sn, which was responsible for increasing the solar cell efficiency to 7.54%.

5. ACKNOWLEDGMENTS

The authors would like to acknowledge the Brazilian research agency Coordenação de Aperfeiçoamento de Pessoal de Nível Superior-Capes for the financial support, the Laboratório de Filmes Finos e Energias Renováveis- LAFFER for the assistance throughout the research.

6. BIBLIOGRAPHY

[1] AKSOY, S., POLAT, O., GORGUN, K., *et al*., "Li doped ZnO based DSSC: Characterization and preparation of nanopowders and electrical performance of its DSSC", *Physica E,* v.121, pp.114127, 2020.

[2] LAI, F., YANG, J., HSU, Y., *et al*, "Enhanced omnidirectional light harvesting in dye-sensitized solar cells with periodic ZnO nanoflower photoelectrodes", *Journal of Colloid and Interface Science,* v. 562, pp. 63–70, 2020.

[3] JUNG, K., LIM, T., MARTINEZ-MORALES, A.A., "CuO shell as a protective layer to improve the stability of ZnO nanorods-based photoelectrode in DSSCs", *Applied Surface Science*, v. 507, pp.144510, 2020.

[4] DAS, A., WARY, R., NAIR, R.G., "Cu modified ZnO nanoflakes: An efficient visible light-driven photocatalyst and a promising photoanode for dye sensitized solar cell (DSSC)", *Solid State Science*, v. 104, pp. 106290, 2020.

[5] IWANTONO, I., SAAD, S.K.M., YUDA, R., *et al.*, "Structural and properties transformation in ZnO hexagonal nanorod by ruthenium doping and its effect on DSSCs power conversion efficiency", *Superlattices and Microstructures*, v. 123, pp. 119-128, 2018.

[6] SINHA, D.D., GOSWAMI, D., AYAZ, A., "Fabrication of DSSC with Nanostructured ZnO Photo Anode and Natural Dye Sensitizer", *Materials Today: Proceedings*, v.5, pp. 2056-2063, 2018.

[7] RAJAN, A.K., LOUIS, C., "Localized surface plasmon resonance of Cu-doped ZnO nanostructures and the material's integration in dye sensitized solar cells (DSSCs) enabling high open-circuit potentials", *Journal of Alloys and Compounds*, v. 829, pp.154497, (2020).

[8] RAHMAN, M.U., WEI, M., XIE, F., *et al.,* "Efficient Dye-Sensitized Solar Cells Composed of Nanostructural ZnO Doped with Ti", *Catalysts*, v.9, pp. 273, 2019.

[9] KHADTARE, S., PATHAN, H.M., HAN, S., *et al.,* "Facile synthesis of binder free ZnO and its Indium, Tin doped materials for efficient dye sensitized solar cells", *Journal of Alloys and Compounds*, v. 872, pp.159722, 2021.

[10] THIRUMOORTHI, M., PRAKASH, J.T.J., "Doping effects on physical properties of (1 0 1) oriented tin zinc oxide thin films prepared by nebulizer spray pyrolysis method", *Materials Science & Engineering B* v. 248, pp. 114402, 2019.

[11] ÖZGÜR, M., PAT, S., MOHAMMADIGHAREHBAGH, R., *et al.* "Sn doped ZnO thin film deposition using thermionic vacuum arc technique", *Journal of Alloys and Compounds* v.774 , pp. 1017-1023, 2019.

[12] XU, L., ZHENG, G., XIAN, F., *et al.* "The morphological evolution of ZnO thin films by Sn ions doping and its influence on the surface energy and photocatalytic activity", *Materials Chemistry and Physics*

v. 229 pp. 215-225, 2019.

[13] YILDIZ, A., SERIN, T., ÖZTÜRK, E., *et al.* "Barrier-controlled electron transport in Sn-doped ZnO polycrystalline thin films", *Thin Solid Films* v. 522, pp. 90–94, 2012.

[14] WIDIYANDARI, H., WIJAYANTI, S., PRASETIO, A., *et al.* "ZnO hollow sphere prepared by flame spray pyrolysis serves as an anti-reflection layer that improves the performance of dye-sensitized solar cells", *Optical Materials* , v.107, pp. 110077, 2020.

[15] AMEEN, S., AKHTAR, M.S., SEO, H., *et al.* "Influence of Sn doping on ZnO nanostructures from nanoparticles to spindle shape and their photoelectrochemical properties for dye sensitized solar cells", *Chemical Engineering Journal* ,v.187, pp. 351-356, 2012.

[16] JUNLABHUT, P., MEKPRASART, W., NOONURUK, R., *et al.* "Characterization of ZnO:Sn nanopowders synthesized by co-precipitation method" *Energy Procedia*, v. 56, pp. 560 – 565, 2014.

[17] AJILI, M., CASTAGNÉ, M., TURKI, N., K., "Study on the doping effect of Sn-doped ZnO thin films", *Superlattices and Microstructures,* v.53, pp. 213-222, 2013.

[18] VISHWAS, M., RAO, K.N., GOWDA, K.V.A., *et al.* "Influence of Sn doping on structural, optical and electrical properties of ZnO thin films prepared by cost effective sol–gel process", *Spectrochimica Acta Part A: Molecular and Biomolecular Spectroscopy* , v. 95, pp. 423–426, 2012.

[19] BEDIA, A., BEDIA, F.Z., AILLERIE, M., *et al.* "Influence of the thickness on optical properties of sprayed ZnO hole-blocking layers dedicated to inverted organic solar cells", *Energy Procedia,* v.50, pp. 603-609, 2014.

[20] LI, S., YAO, C., HAN, Y., *et al.* "Synthesis, electrical and ultrafast nonlinear optical properties of Sn–ZnO composite film", *Optical Materials*, v. 96, pp. 109329, 2019.

[21] CHAHMAT, N., HADDAD, A., AIN-SOUYA, A., *et al.* "Effect of Sn Doping on the Properties of ZnO Thin Films Prepared by Spray Pyrolysis", *Journal of Modern Physics*, v.3, pp.1781- 1785, 2012.

[22] GANESH, V., YAHIA, I.S., ALFAIFY, S., *et al.* "Sn-doped ZnO nanocrystalline thin films with enhanced linear and nonlinear optical properties for optoelectronic applications", *Journal of Physics and Chemistry of Solids*, v.100, pp. 115-125, 2017.

[23] KHELLADI, N.B., SARI, N.E.C., "Optical properties of ZnO thin film", *Advances in Materials Science*, v.13, pp. 22-29, 2013.

[24] ABA-GUEVARA, C.G., MEDINA-RAMÍREZ, I.E., HERNÁNDEZ-RAMÍRES, A., *et al.* "Comparison of two synthesis methods on the preparation of Fe, N-Co-doped TiO2 materials for degradation of pharmaceutical compounds under visible light", *Ceramics International,* v.43, pp. 5068–5079, 2017.

[25] CHONGSRI, K., BANGBAI, C., TECHITDHEERA, W., *et al.* "Characterization and Photoresponse Propreties of Sn-doped ZnO Thin Films", *Energy Procedia*, v. 34, pp. 721–727, 2013.

[26] KANNAN, S., SUBIRAMANIYAM, N.P., LAVANISADEVI, S.U., "Controllable synthesis of ZnO nanorods at different temperatures for enhancement of dye-sensitized solar cell performance", *Materials Letters,* v. 274, pp. 127994, 2020.

[27] YE, N., QI, J., QI, Z., *et al.* "Improvement of the performance of dye-sensitized solar cells using Sn-doped ZnO nanoparticles", *Journal of Power Sources*, v. 195, pp. 5806–5809, 2010.

[28] SOUZA, A.P.S., FERREIRA, O.P., NUNES, V.F., *et al.* "Performance Evaluation of Titanate Nanotubes and Nanoribbons Deposited by Electrophoresis in Photoelectrodes of Dye-Sensitized Solar Cells", Materials Research, v.21 (4), 2018.

[29] ROY, A., SUNDARAM, S., MALLICK, T.K., "Effect of dye sensitization's temperature on ZnO-based solar cells", *Chemical Physics Letters*, v. 776, pp.138688, 2021.

[30] SHASHANKA, R., ESGIN, H., YILMAZ, V.M., *et al.* "Fabrication and characterization of green synthesized ZnO nanoparticle based dye-sensitized solar cells", *Journal of Science: Advanced Materials and Devices,* v.5, pp.185-191, 2020.

ORCID

Vanja Fontenele Nunes https://orcid.org/0000-0003-2458-5616

Francisco Marcone Lima https://orcid.org/0000-0002-1898-9350

Edwalder Silva Teixeira https://orcid.org/0000-0002-6037-5985

Paulo Herbert França Maia Júnior https://orcid.org/0000-0002-4194-7909
Ana Fabíola Leite Almeida https://orcid.org/0000-0002-8867-5453
Francisco Nivaldo Aguiar Freire https://orcid.org/0000-0001-5449-2635